A NOVEL KNOWLEDGE-BASED TOOLPATH CONSTRUCTIVE APPROACH FOR DESIGNING HIGH-PRECISION GRADED LATTICE STRUCTURES

Z. Wang*, Y. Zhang†[1], and A. Bernard*

*IS3P, LS2N, CNRS UMR 6004, Ecole Centrale de Nantes, Nantes, France
† ICB-COMM, CNRS UMR 6303, Université de Technologie Belfort-Montbéliard, Sevenans,
France

Abstract

Current part-scale lattice design methods cause accuracy loss and manufacturability uncertainty in AM preparation stages. STL model conversion and slicing can lead to loss of shape accuracy and surface quality, while unqualified toolpaths may cause printing failures, e.g. pores or re-melting in the powder-bed fusion process. Moreover, all these steps are time-consuming due to the large model file. To solve these challenges, this paper proposes a novel knowledge-based toolpath constructive design method to generate high-precision graded lattice unit cells with manufacturability. It integrates implicit modeling, variable distance field, direct slicing and fine toolpath configuration to construct qualified toolpaths without any intermediate steps. To save computation time in part-scale lattice design, predefined different types or sizes of graded lattice unit cells are populated and assembled into a given design space directly. Hence, it has big potential to improve industrial application of part-scale porous structures with fine and gradient porous features.

Key words: Tool-path; Constructive design; Triply periodic minimal surface; Knowledge-based system.

1. Introduction

Additive manufacturing (AM) technologies have the potential to produce highly complex geometries and material compositions with a layer-by-layer printing strategy enabling to achieve a non-linear relationship between the geometry complexity and manufacturing cost [1-3]. Since the layer construction method is totally different from conventional manufacturing processes, designers and engineers enable to use intricate structures, e.g. triply periodic minimal surface (TPMS), to have more freedom in product design, such as tissue engineering [4] and heat sink [5]. As AM technology becomes more mature, it is possible to fabricate metal parts with high-precision complex geometry and extremely fine features, especially using the laser powder bed fusion (L-PBF) process. However, high manufacturing precision also leads to more preparation time in AM processing chain. In addition, Boolean operations would cause a large computing time and data storing space while generating high-precision TPMS-based porous structures. In particular, with the increase of the CAD model size, these issues make fabrication of part-scale porous structures become more and more difficult.

To avoid the loss of accuracy and efficiency issues, this paper proposes a knowledge-based toolpath configuration method, where a set of toolpath patterns are pre-defined for different types and sizes of uniform or graded TPMS structures with ensured manufacturability. The proposed method can

---

[1] Corresponding author. E-mail: yicha.zhang@utbm.fr

significantly simplify the conventional toolpath generation method without any solid-related representation. With an implicit modeling and distance field, different types of graded offset TPMS surfaces can be created directly. Different types of toolpath patterns are infilled within slice contours via directly slicing the offset surfaces. Taking into account the repeated appearance of same-size lattice unit cell, the lattice unit with the same gradient thickness information is defined and stored in a knowledge-based data set.

The remaining contents are organized as follows: the related work will be presented in Section 2; Section 3 will introduce the proposed method; Cased study in the section 4 will be given for method demonstration, and Section 5 ends with a conclusion and future research perspectives.

2. Related work

Lightweight TPMS lattice structures has gained attention due to the attractive internal intricate structures. Currently, the methods to print part-scale lattice or porous structures usually follow the traditional design and printing preparation method. At first, a CAD model or design domain filling with complex lattice unit cells is designed by conventional CAD tools. Then, the CAD model obtained is converted into a Stereo-lithography (STL) file that can be recognized by many AM machines' preparation software tools. In general, it will cause the loss of geometrical accuracy in the model manipulation and conversion. Then, the mesh file is processed by a preprocessing software to obtain a slicing model. It is also easy to lead to accuracy loss in the cross-sections from STL model to slicing model, especially for fine porous TPMS structures. In the end, different types of toolpath patterns are infilled within the layers of a slicing model. The infilling process usually causes additional accuracy loss when facing shapes with concave contours since toolpaths at those locations may have overlaps or voids. Hence, the generated toolpaths should be validated before printing in real manufacturing context. Currently, the preparation process in traditional AM processing chain can be summarized as CAD model building, STL file conversion, and toolpath infill before printing. These three stages will not only cause the loss of geometrical accuracy, but also consume much computational time and memory for part-scale porous structure design. Moreover, it becomes worse when using intricate TPMS structures to infill within the part-scale lattice structures. Fig. 1 shows the main steps for designing graded TPMS structures.
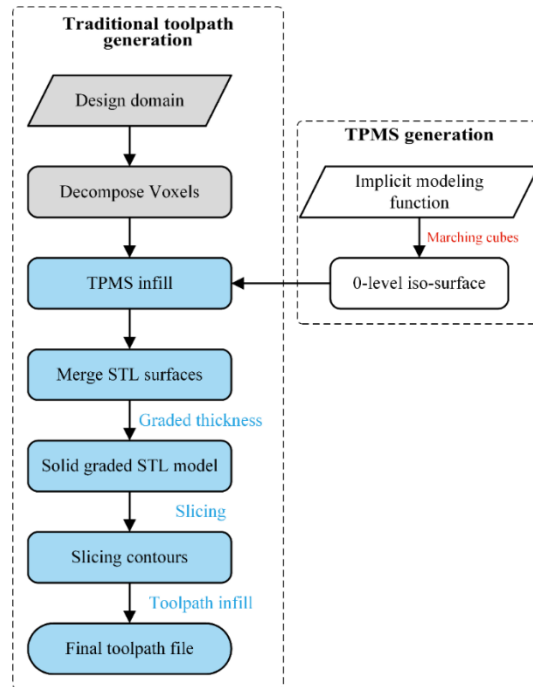
Fig. 1. Traditional toolpath generation method for graded TPMS-based porous structures.

In literature, many studies were proposed to improve the efficiency and precision issues of part-scale lattice structure designs. To avoid slicing the solid TPMS model, Feng et al. [6] proposed to use the Marching Square (MS) algorithm to slice open-surface TPMS structures directly. Then, based on the uniform thickness information, a bidirectional-offset-union strategy was developed to generate valid toolpath infill. However, it is still costly to deal with part-scale lattice design issues using the solid-free method. In addition, the proposed method can only construct TPMS structure with uniform thickness. Another STL-free design method was proposed by Ding et al. [7]. Implicit solid modeling and direct slicing method are used to construct toolpath configuration. Hence, it can ensure a high-precision toolpath infill for the powder bed fusion process when fabricating multi-level TPMS structures. However, the STL-free method has difficulty handling complex graded TPMS structures. In addition, the cost of slicing and toolpath generation was omitted in the implicit method. The toolpath configuration is still conducted for the whole part model. Ponche et al. [8] proposed a novel methodology of design for AM to optimize the part geometry from toolpath directly. Hence, it provided a new horizon to bridge the gap between CAD model and the corresponding manufactured part. Inspired by the pioneering work [8], a new toolpath-based layer construction method is proposed to design micro-scale porous structures in [9]. The proposed method can save time in design and printing preparation with ensured manufacturability. The toolpath is defined implicitly and the travel path is also optimized to guide the laser trajectory.

To summarize, current TPMS-based lattice design methods have the following problems: **a.** it is difficult to improve computational efficiency when dealing with part-scale lattice structures. **b.** it is hard to ensure the accuracy while designing graded TPMS structures. To solve these problems, the manuscript attempts to propose a new knowledge-based toolpath constructive solution.

3. Proposed method

3.1. Method overview

Different from the traditional CAD-STL-Slice-Toolpath modeling, the proposed method uses solid-free modeling method to generate toolpath configuration directly. Fig. 2 shows the proposed knowledge-based toolpath configuration method for designing graded TPMS-based porous structures.
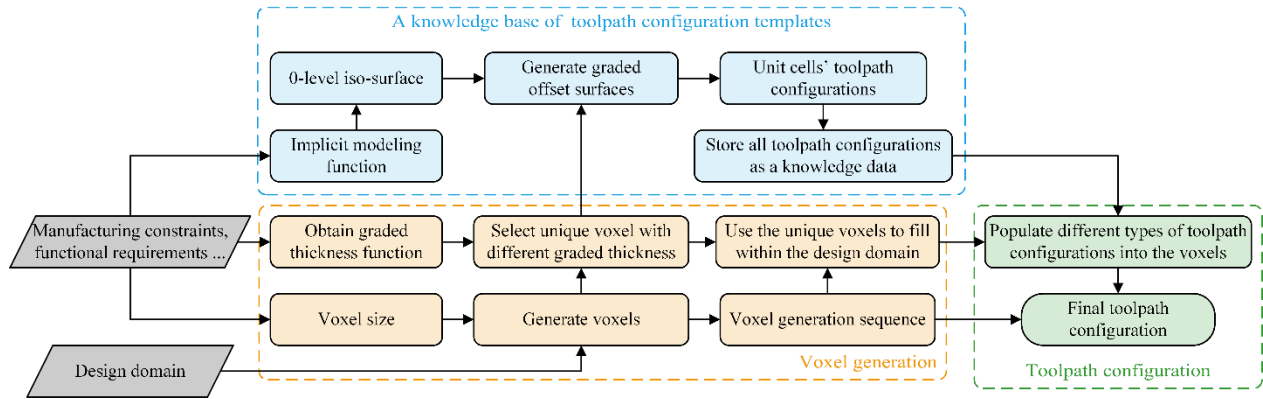

Fig. 2. Flowchart of the proposed knowledge-based toolpath configuration method for designing graded TPMS-based porous structures.

The proposed method has three modules to manage the toolpath configuration. First, a given design domain is decomposed into voxels based on certain requirements, e.g. manufacturing constraints or functional requirements, as shown in Fig. 3. Here, we suppose that all voxels have the same size and are filled with the same type of lattice unit cell. In this process, the fabrication sequence can be also defined to facilitate the toolpath configuration for voxels in different positions. Then, according to the graded thickness, unique voxels with different graded thickness information are selected to serve for graded offset surfaces generation.
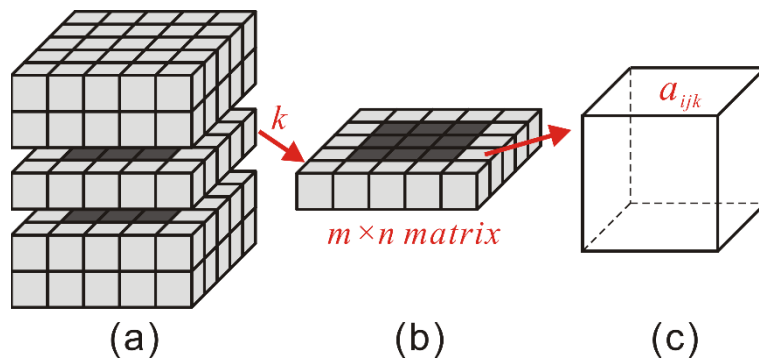

Fig. 3. Voxel decomposition process: (a). Voxel representation in a three-dimensional matrix; (b). A two-dimensional matrix; (c). A voxel a_{ijk}.

In the module of the knowledge data for unit cells' toolpath configuration, an implicit function is used to create 0-level iso-surface via the Marching Cubes (MC) algorithm [10]. According to thickness information of different voxels, offset surfaces are built by using different distance field functions. Then, toolpaths are populated into the area between two offset surfaces directly. Moreover, different types of toolpath patterns are utilized to infill the slice contours. At the same time, the travel path can be also defined in the toolpath configuration. Finally, these toolpath configuration units are as infilling templates, filling knowledge units, which can be selected to infill the voxels.

In the third module, the toolpath information stored in the templates is selected to populate for reproduction into the voxels (a_{ijk}) of different positions. In addition, the scanning sequence and path of multiple lasers can also be assembled into the output file of final toolpath configuration. By using the proposed knowledge-based toolpath configuration method, computational time and memory can be saved significantly.

3.2. TPMS structure generation

The implicit method uses a single-value function of three variables to describe approximated TPMS with periodic surfaces [11]. Three common TPMS structures, Schwarz Primitive, Diamond and Schoen Gyroid surfaces can be expressed by the following nodal equations:

$$\phi_P(x, y, z) = \cos(\omega x) + \cos(\omega y) + \cos(\omega z) = C$$
$$\phi_D(x, y, z) = \cos(\omega x - \omega y)\cos(\omega z) + \sin(\omega x - \omega y)\sin(\omega z) = C \quad (1)$$
$$\phi_G(x, y, z) = \cos(\omega x)\sin(\omega y) + \cos(\omega y)\sin(\omega z) + \cos(\omega z)\sin(\omega x) = C$$

Where x, y, z are the spatial coordinates, $\omega = 2\pi / L$ and L is the size of the lattice unit cell, C can control the surface expansion. The surface Γ, a zero-level set of Φ, represents the interface regions which divide the unit cell into two distinct spaces. Fig. 4 shows the three TPMS structures accomplished with the polygonization of Γ by using the MC algorithm.

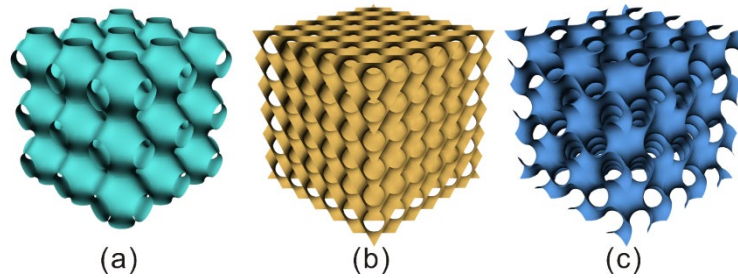

(a)   (b)   (c)

Fig. 4. Different types of TPMS structures (3*3): (a). Schwarz Primitive surface; (b). Schwarz Diamond surface; (c). Schoen Gyroid surface.

In order to explain the 3D MC algorithm, the MS algorithm in 2D is illustrated in Fig. 5. The MS algorithm is used to provide a piecewise-line approximation to a 2D object [12]. To describe an implicit function, the design domain is divided into a 2D grid. Each nodes of the grid can be calculated by the implicit function. Fig. 5(a) enumerates all 16 intersection situations, which show the representations of all lines in the 2D space. Hollow and solid points indicate the position of the grid

$f(p_1) < 0, f(p_2) > 0, f(p_3) < 0, f(p_4) < 0$ with $f(p)$ being the value of the implicit function on each node. To extract the line from the square, valid grid edges need to be detected. For a valid edge, the grid nodes p_i and p_{i+1} should satisfy the following:

$$f(p_i)f(p_{i+1}) < 0 \tag{2}$$

Hence, two valid edges in Fig. 5(b) are $p_1 p_2$ and $p_2 p_3$. The intersection P can be calculated via the linear interpolation approach as

$$f((1-\alpha)p_i + \alpha p_{i+1}) = 0 \tag{3}$$

Based on the intersection situations of the MS algorithm, the connection of all intersection P can be determined to construct an approximate 0-iso-line. The resolution of the grid can be improved to obtain a high-precision 0-iso-line.
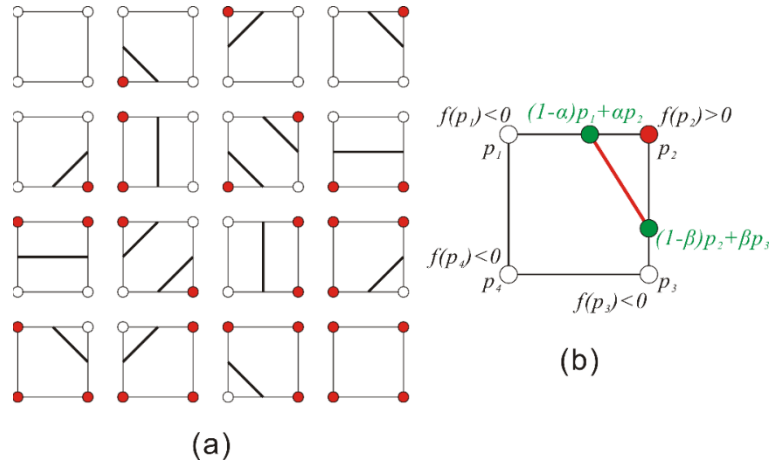

Fig. 5. (a). All configurations of the MS algorithm; (b). The linear interpolation method for a square.

3.3. Graded offset TPMS generation

In this subsection, a MC-based distance field method is proposed to generate graded TPMS offset surfaces. In the proposed method, the 0-iso-level surface (H

H is a mesh surface that can be controlled by the resolution of the MC algorithm. Then, the closest distance between uniform points P from the MC algorithm and the surface H can be represented as $dis(p, \partial H)$, and the corresponding closet points on the surface are described as P_H. Since we have an implicit graded thickness function T_G, the thickness values in P_H can be represented as T_{PH}. Hence, the distance field for the point set P can be described as

$f(p) = dis(P, \partial H) - T_{PH}$. The distance field will be used as an input of the MC algorithm to obtain the graded TPMS surface. Fig. 6 shows the flowchart.
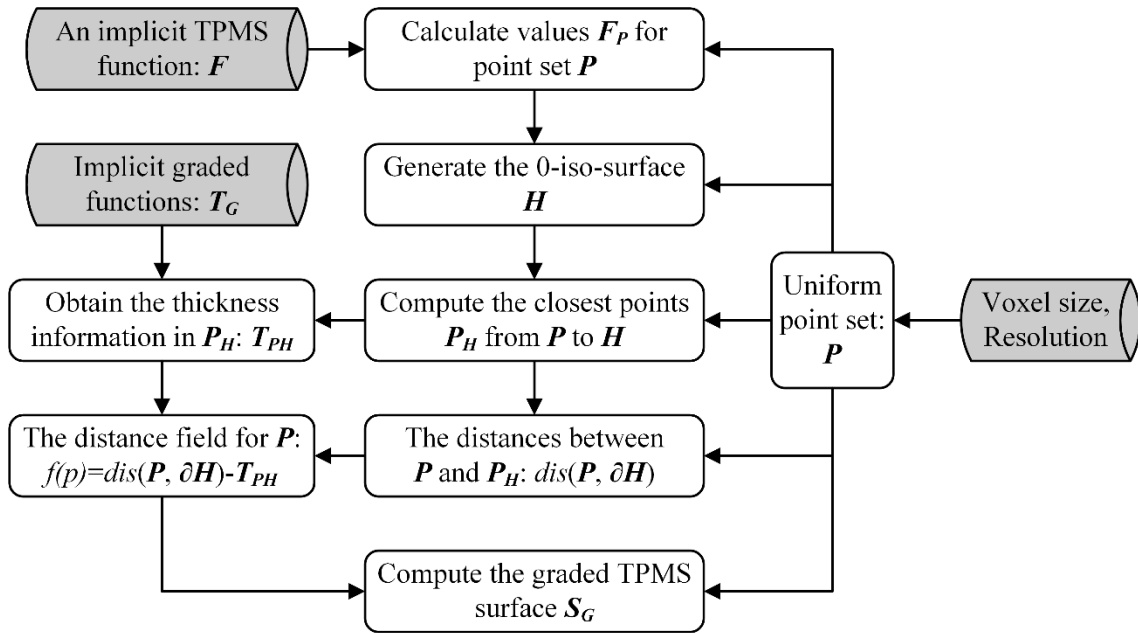

Fig. 6. The flowchart of the graded TPMS surface generation method.

An implicit cylinder example ($x^2 + y^2 - 9 = 0$) is used to explain the method in Fig. 7. For grid points with iso-surface values greater than zero, these points lie outside of the circle. All those with negative values lie inside of it. In order to generate an offset surface, a distance field is used to measure the distance between grid points and the mesh surface. The distance field can be described by the following equation [13]:

$$f(p) = dis(p, \partial H) - r \qquad (4)$$

Where p are the grid points and H is the given cylinder generated by the MC algorithm. The distance field represents the minimum distance from these grids to the given model. For these points outside H, the function will return the distance with positive. The distance values are seen as negative for these points inside. Hence, the offset value r can be either negative or positive.
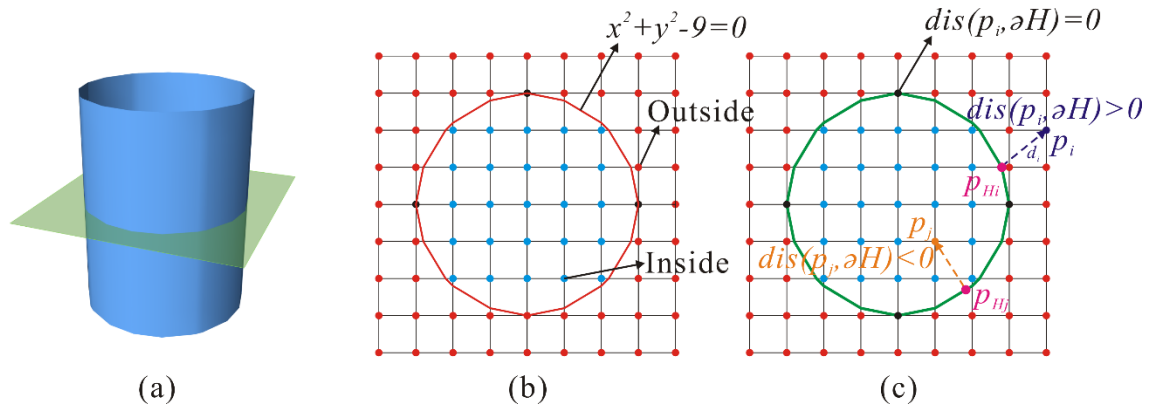
Fig. 7. An implicit cylinder generation using Marching Cubes algorithm in 2D.

To explain it easily, Fig. 8 show the generation of the inside and outside offset cylinder in 2D. To generate an offset cycle, an offset value is needed to calculate the distance field. Here, the offset value is set as $r = \pm 1$. The distance field is computed to return the MC algorithm. Two offset circles in 2D are shown in Fig. 8.
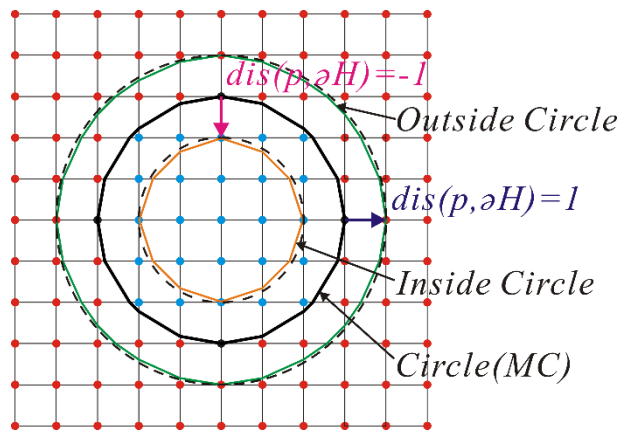

Fig. 8. The representation of the inside and outside offset circles.

The distance field function can also be used to generate a graded offset surface by describing a thickness field based on geometry information. For example, a distance field of deformed circles can be expressed as:

$$f(p) = dis(p_i, \partial H) \pm (\frac{p_i^x}{6} + 1) \tag{5}$$

Where p_i^x is the x-axis coordinate of point p_i. Fig. 9 shows two graded offset circles via a graded thickness filed. Hence, the proposed method can be also applied to generate offset TPMS surfaces.
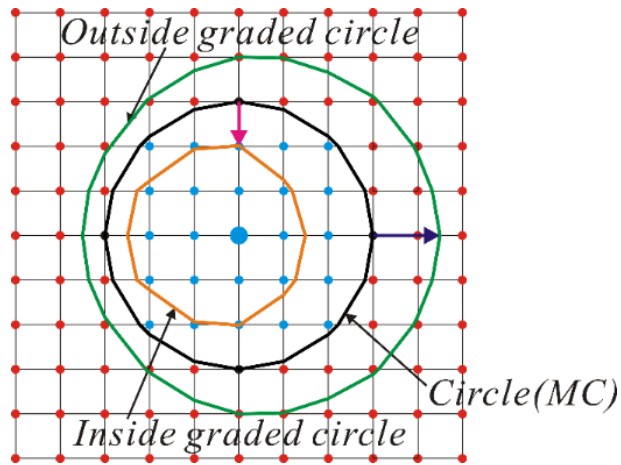
Fig. 9. Graded offset circles generation.

By adjusting the resolution of the MC algorithm, the precision of graded offset surfaces can be controlled. To describe the impact of resolution, a sphere is represented using the MC algorithm. The mathematical expression is defined by:

$$f(S) = \sqrt{x^2 + y^2 + z^2} - R \tag{6}$$

Where x, y, z are the spatial coordinates and R represents the radius of the sphere. The radius is defined as 3 mm. Fig. 10 shows different spheres with different resolutions.
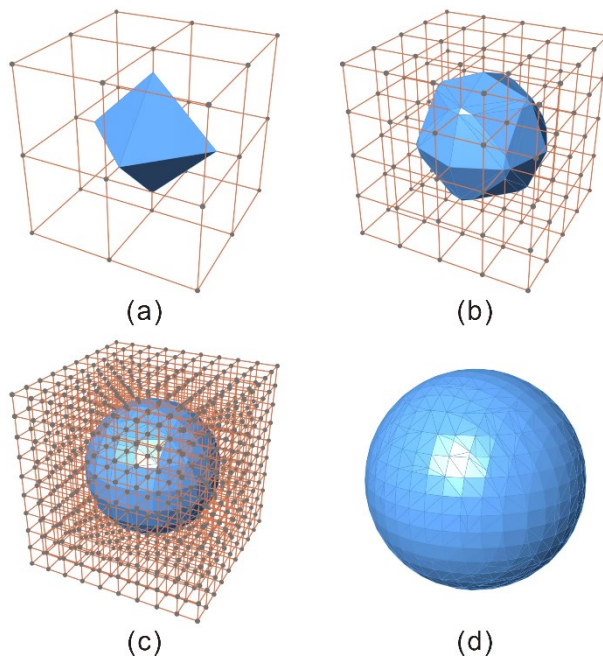

Fig. 10. Different spheres with different resolution setting: (a). resolution = 3; (b): resolution = 5; (c). resolution = 10; (d). resolution = 20.
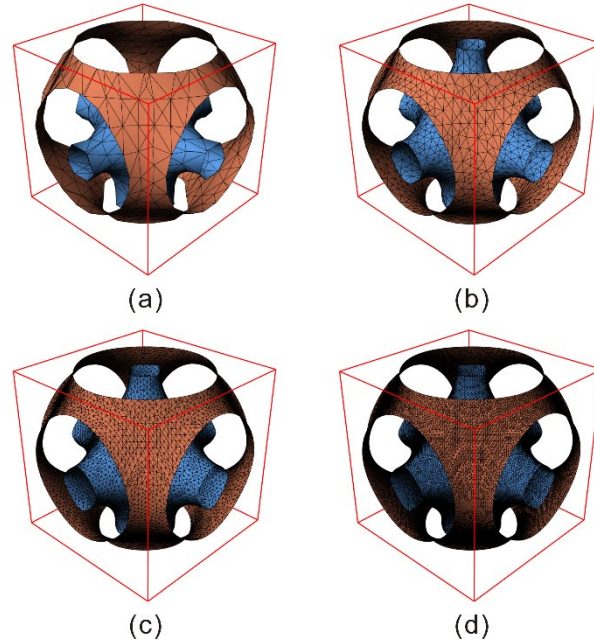
Fig. 11. TPMS surfaces with different resolution settings: (a). resolution = 10 ($V_I = 260$, $F_I = 478$; $V_O = 336$, $F_O = 520$); (b): resolution = 20 ($V_I = 1220$, $F_I = 2328$; $V_O = 1348$, $F_O = 2376$); (c). resolution = 40 ($V_I = 5052$, $F_I = 9856$; $V_O = 5340$, $F_O = 10000$); (d). resolution = 80 ($V_I = 20596$, $F_I = 40680$; $V_O = 21136$, $F_O = 40904$).

In addition, due to the high manufacturing accuracy of the SLM process, the surface precision of fine TPMS lattice structures is required to be smoother. The proposed method can ensure the TPMS lattice structure model with a high-precision surface accuracy via a high resolution setting. Fig. 11 compares the effect of different resolutions on the sizes of STL files. As the resolution of STL files increases, the number of faces and vertices of the triangular mesh increases exponentially. In general, high-precision STL files lead to an increase in pre-processing time and a large consumption of computational memory.

3.4. Toolpath infill for graded offset surfaces

As mentioned above, the MC-based distance field can construct offset surfaces with different gradients for a TPMS unit cell. A solid-free toolpath configuration method is developed in this subsection. The proposed method allows us to slice offset surfaces directly. Meanwhile, to avoid time consumption in AM preparation stages, the toolpath result obtained is stored in a knowledge base for the subsequent toolpath configuration. Fig. 12 give a workflow of the toolpath configuration generation method for a graded TPMS-based unit cell example.

1194

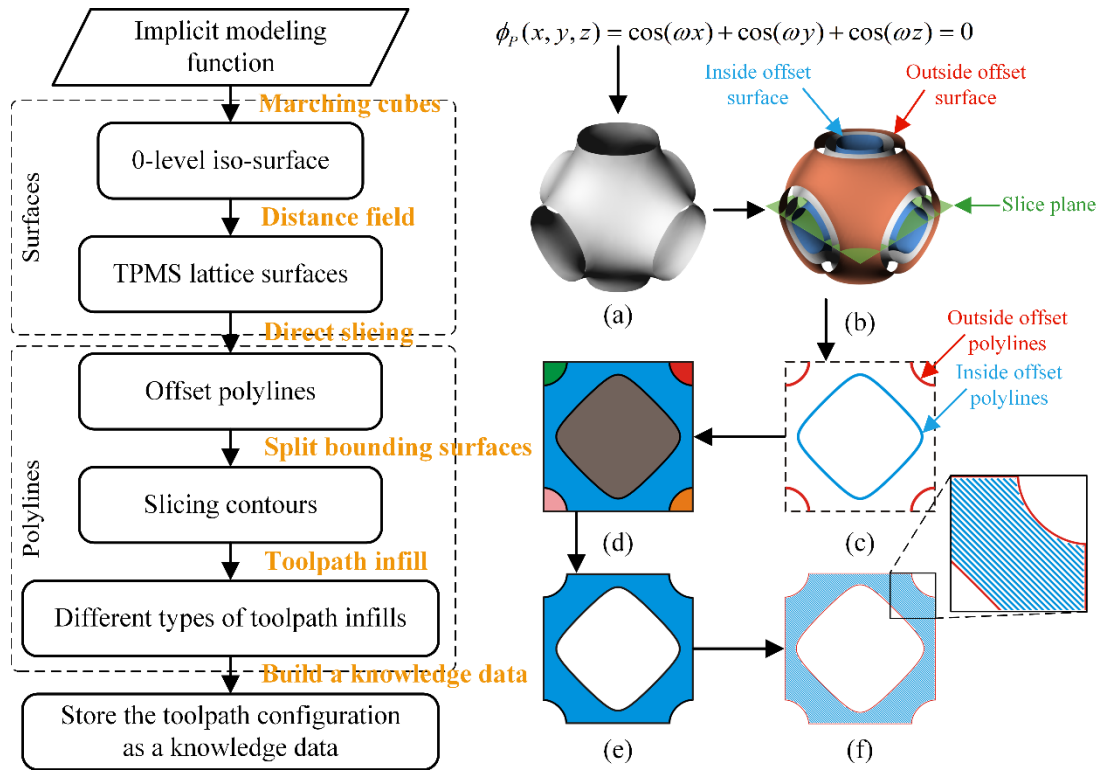$$\phi_P(x, y, z) = \cos(\omega x) + \cos(\omega y) + \cos(\omega z) = 0$$

Fig. 12. Workflow of toolpath configuration generation for a graded TPMS-based unit cell example.

By using the MC-based distance field, graded offset surfaces are obtained. The surface precision can be adjusted by changing the resolution of x, y, and z in the voxel. Fig. 12(b-f) show the main steps of the direct slicing method. A slice plane in Fig. 12(b) is applied to slice the offset surfaces. The distance between two adjacent slice planes should respect the layer thickness. Two kinds of intersection polylines, called outside and inside offset polylines, are obtained to split the bounding surface in Fig. 12(c, d). The surface enclosed by the two intersection polylines is the slicing contour. Different types of toolpaths can be used to populate within the slicing contour.
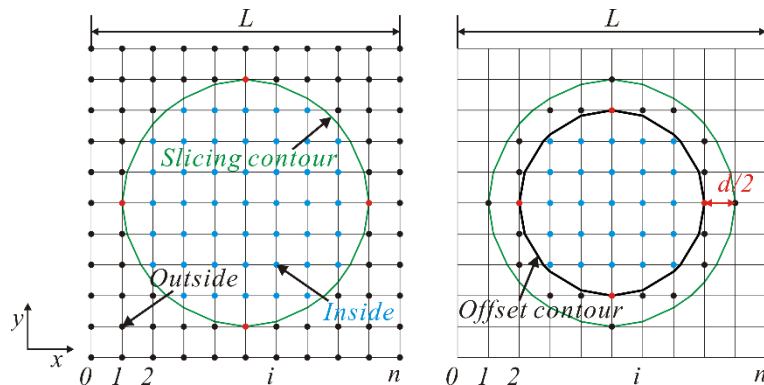

Fig. 13. Resolution definition of intersection-free contour based on the hatch spacing.
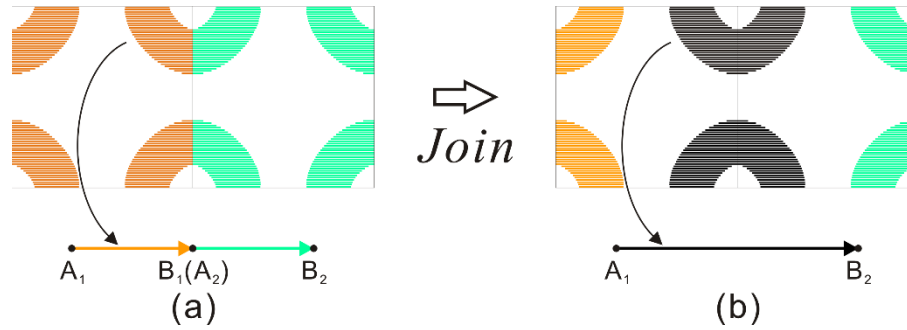
Fig. 14. Adjacent joined zigzags in different voxels.

For the L-PBF process, there are generally two types of scans: contour and infill. The contour scan is usually used to scan the boundaries and the infill scan is used to scan across all areas. The zigzag scan is one of the most common infill scanning strategy in the literature. The scanning strategy plays an important role in microstructures, mechanical properties, and residual stresses of AM parts [14]. To form the large-size parts with high quality, the island scanning strategy is seen as an alternative method to avoid excessive and accumulated stress [14]. Since the proposed method enables to manipulate toolpaths directly, contour and zigzag scanning strategies are used to construct toolpath knowledge bases. To ensure the manufacturability of the contour toolpath, the MS algorithm is used to generate intersection-free contours [13]. The detailed method can be seen in Fig. 8. Notice that resolution should respect the following expression to ensure the qualified intersection-free contour generation in Fig. 13.

$$L \leq n\frac{d}{2} \tag{7}$$

Where L is the size of the voxel, n represents the resolution of the MS algorithm, and d is the hatch spacing of an AM processing. In Fig. 12(f), a contour pattern is used to scan the boundary of the slice contour and parallel-vector toolpath is filled within the contour pattern. This combined toolpath configuration is more suitable for the island scanning technique. In addition, the zigzag scanning strategy can be used alone. In this situation, adjacent zigzags in different voxels can be joined together as shown in Fig. 14.

Taking into account that many part-scale lightweight structures with TPMS sheet usually use the same type and size lattice unit cell, the toolpath configuration for a single TPMS lattice unit cell can be seen as a knowledge data set, parametric template, stored in a knowledge-based system. Therefore, a set of toolpath configurations for graded TPMS unit cells can be predefined and stored in a knowledge base. It means that the proposed knowledge-based toolpath configuration method allows us to populate predefined toolpath configuration into voxels directly and generate 3D toolpath model to approaching the desired CAD model in an implicit way, which is similar to the proposed toolpath construction method in [9]. To achieve different kinds of scanning strategies, the infilled toolpaths can be analyzed further. In addition, the proposed method can ensure the manufacturability of high-precision toolpaths given a high resolution for the MC and MS algorithms since qualified toolpath patterns for infilling can be predefined in the knowledge base.

4. Case study

In this section, two types of TPMS unit cells, Schwarz P surface and OCTO surface are used to generate toolpath configurations directly for implicitly designing graded high-precision TPMS structures. Table 1 gives a process parameter definition.

Table 1. Process parameter definition

Voxel size L (mm)	Layer thickness t (μm)	Hatch spacing d (μm)
2*2*2	40	50

To generate a graded Schwarz P structure, a graded thickness function is proposed in the following:

$$t_z^P = \pm \frac{1}{10}\left(2\sin\frac{\pi(p_z+1)}{4}+1\right), \ (-1\le p_z<1) \tag{8}$$

Where t_z is the thickness of the graded surface along z direction, p_z is the coordinate value of points on the standard Schwarz P surface. The MC algorithm is used to generate the standard P surface with the $150\times150\times150$ resolution. Fig. 15 shows the three kinds of P surfaces and their combination.
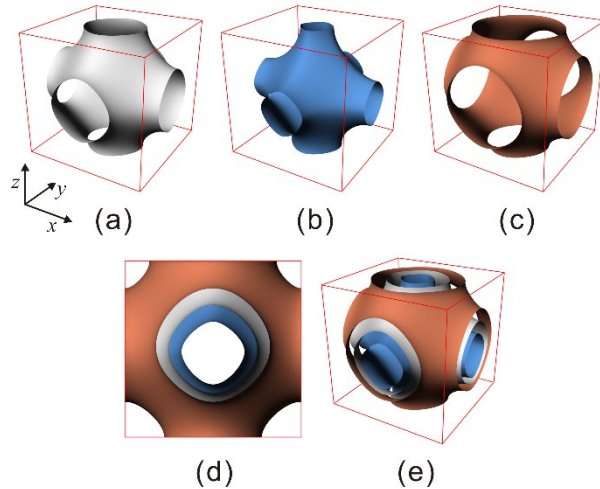

Fig. 15. Graded offset P surface generation: (a). standard P surface; (b). inside offset surface; (c). outside offset surface; (d). front view of the three surfaces; (e). perspective view.

Two parallel-vector scanning strategies, island and continuous strategies, are applied to construct toolpath configurations for the graded P structure. Fig. 16 presents the two parallel-vector techniques with island and non-island scanning modes. A $90°$ rotation with x axis in scan orientation is performed after each layer. For the island scanning mode, unjoined toolpath configurations are filled within the voxel directly. For the parallel-vector technique, the toolpaths of mutual contact between two adjacent voxels are joined together, as shown in the right of Fig. 16.
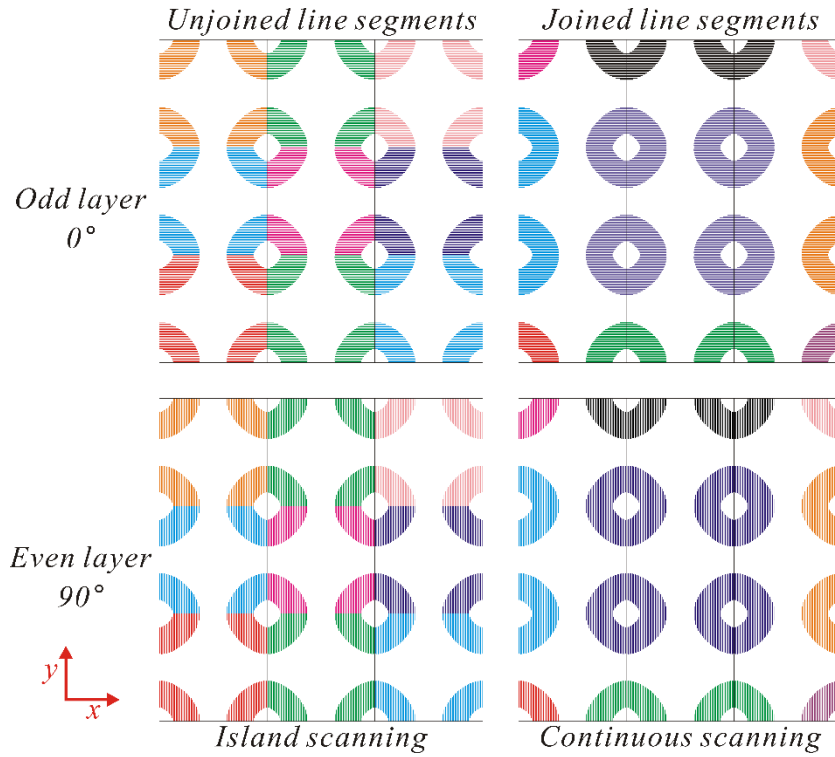
Fig. 16. Two parallel-vector scan strategies of the alternative layers

In addition, the contour scan is also performed in the toolpath configuration. Fig. 17 presents the toolpath in the layer 24 and 25. A $67°$ rotation with initial angle $45°$ is conducted in this scanning mode.

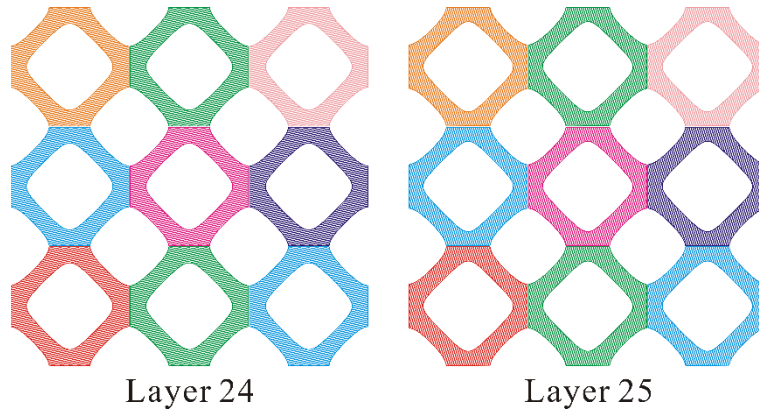Layer 24   Layer 25

Fig. 17. Contour and parallel-vector scanning modes in two layers.

Another graded thickness function is utilized in the OCTO surface as follows:

$$t_z^{OCTO} = \pm\frac{1}{20}\left(2\sin\frac{\pi(p_z+1)}{4}+1\right), \ (-1 \le p_z < 1) \tag{9}$$
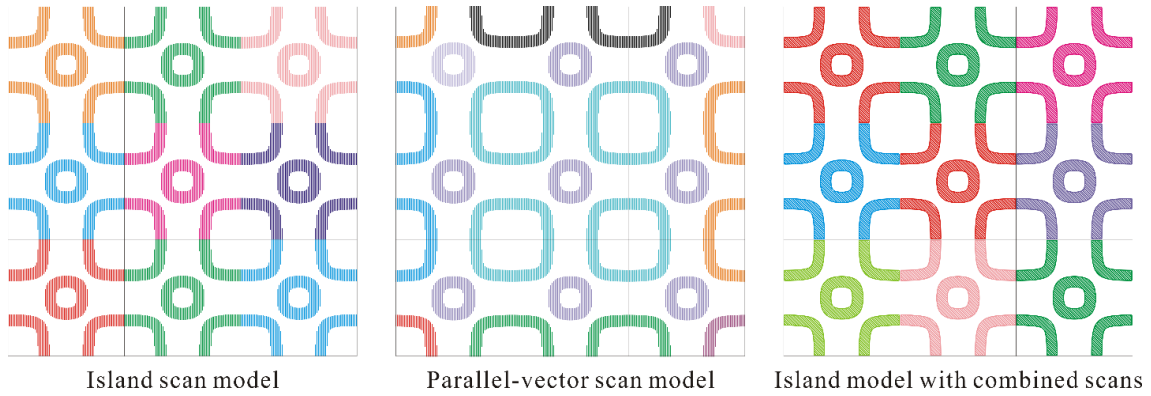
Fig. 18. Three scanning strategies with $90°$ related to x-axis.

Three scanning strategies, island with parallel-vector, parallel-vector and island with combined scans are used to generate toolpath configurations for each graded TPMS unit cells. The three strategies are shown in Fig. 18.
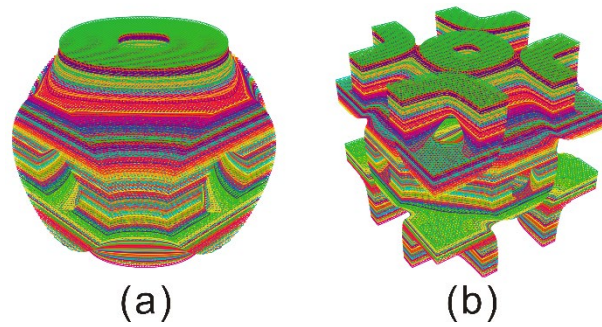

Fig. 19. Two toolpath configurations for graded P and OCTO structure unit cells.

Here, we use the island scanning strategy with contour and parallel-vector modes to construct toolpath configurations for the two graded TPMS structures as shown in Fig. 19.
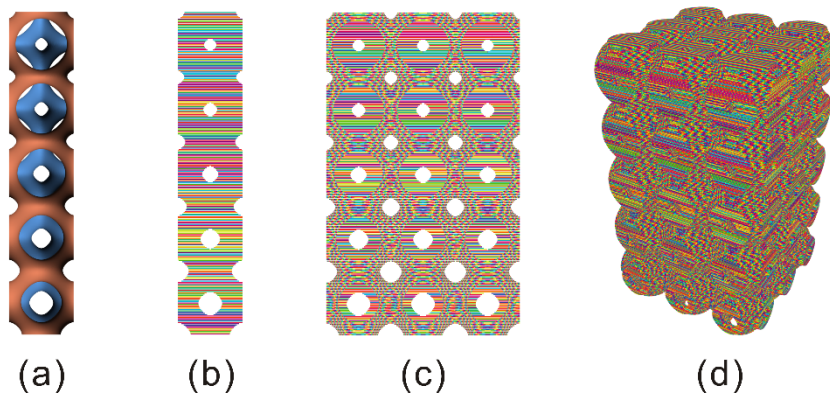

Fig. 20. A graded toolpath configuration assembly along *z* direction: (a). graded offset surfaces; (b). graded toolpath configurations of unique voxels; (c). front view of the toolpath assembly; (d). perspective view of the assembly.

1199

To assemble a final toolpath configuration of a part-scale graded structure, Fig. 20 shows a graded toolpath configuration assembly along *z* direction.

5. Conclusion and future research perspectives

The proposed knowledge-based toolpath constructive method can design graded TPMS structures more efficiently with qualified toolpaths and robust manufacturability. It has more potential to become a new digital framework for design complex uniform or graded porous structures with greatly reduced geometric modeling time and printing preparation time and improve printing accuracy since there is neither CAD modeling nor meshing where accuracy loss happens. In the future, the proposed knowledge-based method will be validated for the L-PBF process to fabricate fine porous gradient structures that are needed in diverse applications. Then, more TPMS structures and toolpath patterns will be benchmarked in experiments to help construct qualified toolpath pattern knowledge bases for configuration design. Moreover, the authors would like to exploit more applications in multi-material and 4D printing designs, where direct writing methods, which are convenient for defining toolpath construction rules, are widely used.

Reference

[1] Thompson M.K., Moroni G., Vaneker T., Fadel G., Campbell R.I., Gibson I., Bernard A., Schulz J., Graf P., Ahuja B., Martina F., Design for Additive Manufacturing: Trends, opportunities, considerations, and constraints, CIRP Annals, 65 (2016) 737-760.
[2] Lebaal N., Zhang Y., Demoly F., Roth S., Gomes S., Bernard A., Optimised lattice structure configuration for additive manufacturing, CIRP Annals, 69 (2019) 117-120.
[3] Vaneker T., Bernard A., Moroni G., Gibson I., Zhang Y., Design for additive manufacturing: Framework and methodology, CIRP Annals, 69 (2020) 578-599.
[4] Yoo D.-J., Computer-aided porous scaffold design for tissue engineering using triply periodic minimal surfaces, International Journal of Precision Engineering and Manufacturing, 12 (2011) 61-71.
[5] Catchpole-Smith S., Sélo R.R.J., Davis A.W., Ashcroft I.A., Tuck C.J., Clare A., Thermal conductivity of TPMS lattice structures manufactured via laser powder bed fusion, Additive Manufacturing, 30 (2019).
[6] Feng J., Fu J., Lin Z., Shang C., Niu X., Layered infill area generation from triply periodic minimal surfaces for additive manufacturing, Computer-Aided Design, 107 (2019) 50-63.
[7] Ding J., Zou Q., Qu S., Bartolo P., Song X., Wang C.C.L., STL-free design and manufacturing paradigm for high-precision powder bed fusion, CIRP Annals, (2021).
[8] Ponche R., Kerbrat O., Mognol P., Hascoet J.-Y., A novel methodology of design for Additive Manufacturing applied to Additive Laser Manufacturing process, Robotics and Computer-Integrated Manufacturing, 30 (2014) 389-398.
[9] Zhang Y., Tan S., Ding L., Bernard A., A toolpath-based layer construction method for designing & printing porous structure, CIRP Annals, (2021).
[10] Lorensen W.E., Cline H.E., Marching cubes: A high resolution 3D surface construction algorithm, in: Proceedings of the 14th annual conference on Computer graphics and interactive techniques - SIGGRAPH '87, 1987, pp. 163-169.

[11] Rajagopalan S., Robb R.A., Schwarz meets Schwann: design and fabrication of biomorphic and durataxic tissue engineering scaffolds, Med Image Anal, 10 (2006) 693-712.

[12] Maple C., Geometric design and space planning using the marching squares and marching cube algorithms, in: 2003 international conference on geometric modeling and graphics, 2003. Proceedings, IEEE, 2003, pp. 90-95.

[13] Liu S., Wang C.C., Fast intersection-free offset surface generation from freeform models with triangular meshes, IEEE Transactions on Automation Science and Engineering, 8 (2010) 347-360.

[14] Jia H., Sun H., Wang H., Wu Y., Wang H., Scanning strategy in selective laser melting (SLM): a review, The International Journal of Advanced Manufacturing Technology, 113 (2021) 2413-2435.